

# Performance optimisation of a modified Duck through optimal mass distribution

Jorge Lucas<sup>1</sup>, Stephen Salter<sup>1</sup>, João Cruz<sup>2</sup>, Jamie Taylor<sup>1</sup> and Ian Bryden<sup>1</sup>

<sup>1</sup>Institute for Energy Systems,  
University of Edinburgh,  
EH9 3JL, Edinburgh, UK  
E-mail: J.Lucas@ed.ac.uk

<sup>2</sup>Garrad Hassan Ibérica

## Abstract

A new design for the solo desalination Duck Wave Energy Converter is being studied at the University of Edinburgh. The key innovation is the modification of the profile. A numerical hydrodynamic model showed that similar performance could be obtained by using a circular cylinder with an off-centred axis of rotation. The principle advantage of this new design is the reduction of the cost of the manufacturing process. A 1:33 scale model was built to validate the numerical predictions and has been tested in a wave tank in regular and irregular seas.

The optimisation of the performance of this device requires a systematic investigation of the effect of several variables. In this paper the effect of mass redistribution is analysed. A simplified one degree-of-freedom frequency-domain model with its power-take-off based on linear damping is used and an equation for the position of the ballast mass that maximises the performance of the device for a certain wave exciting frequency is derived.

It is shown that by relocating the ballast (i.e. changing the inertia of the Duck) a new condition that optimises the performance of the device for a particular wave climate is obtained.

**Keywords:** Wave Energy Converters, Edinburgh Duck, WAMIT, optimisation of performance, mass distribution, vapour compression desalination.

## Nomenclature

$\nabla$	= submerged volume
$\alpha$	= angle that defines the position of the axis of rotation (see Figure 7)
$\Delta$	= quantity defined by equation (16d)
$\gamma_0, \gamma_1$	= constants defined by equations (15b) and (15e)
$\omega$	= angular frequency of the incident wave
$\rho$	= density of water
$\psi$	= angular displacement (in pitch)
$\tilde{\psi}$	= complex amplitude of the angular displacement

$a_{55}$	= added mass associated with pitch motion
$b, c$	= quantities defined by equation (16a)
$b_{55}$	= hydrodynamic damping associated with pitch motion
$\vec{b}_j$	= base vectors associated with the body-fixed coordinate system ( $j = 1, 2, 3$ )
$c_{55}$	= hydrostatic stiffness associated with pitch motion
$c_g$	= group velocity of the incident wave
$d_B, d_H$	= distances from the centre of rotation to the centre of mass of the ballast and hull respectively
$\vec{e}_j$	= base vectors associated with an inertial reference frame located at the centre of rotation ( $j = 1, 2, 3$ )
$f_c$	= pitch moment of the hydrostatic stiffness force
$f_d$	= power-take-off moment
$f_h$	= pitch moment of the hydrodynamic force
$f_r$	= pitch moment of the radiation force
$f_X$	= pitch moment of the excitation force
$h$	= draft (see Figure 7)
$i$	= pure imaginary number ( $\sqrt{-1}$ )
$g$	= gravity acceleration constant
$l_0$	= distance between the centre of rotation and the centre of the cylinder
$m$	= total mass of the system
$m_B$	= mass of the ballast
$m_H$	= mass of the hull
$t$	= time variable
$u$	= angular velocity of the Duck
$\dot{u}$	= angular acceleration of the Duck
$x$	= mass ratio between the hull and ballast
$z_0$	= water depth
$z_g$	= centre of mass of the Duck relative to the body fixed coordinate system
$A$	= amplitude of the incident wave
$B$	= point located at the centre of mass of the ballast
$C$	= point located at the centre of the cylinder
$D$	= diameter of the cylinder
$E$	= average energy density of the incident wave
$F_d$	= complex amplitude of the power-take-off force
$H$	= point located at the centre of mass of the hull
$l_0$	= auxiliary constant defined in expression (14f)
$I_B, I_H$	= Inertia at the centre of mass of the ballast and hull respectively (in the direction of $\vec{b}_2$ )
$J_{22}$	= inertia of the Duck at the centre of rotation
$J_B, J_H$	= inertia at the centre of rotation of the ballast and hull respectively (in the direction of $\vec{b}_2$ )
$K_0$	= linear damping associated with the power-take-off
$K_B$	= radius of gyration of the ballast
$\overline{P}_{abs}$	= mean absorbed power
$\overline{P}_{max}$	= maximum mean absorbed power
$\overline{P}_w$	= average power per unit crest length
$R$	= fixed point located at centre of rotation (see Figure 7)
$RCW$	= relative capture width

$T$	= incident wave period
$U$	= complex amplitude of the velocity of the Duck
$V$	= total volume of the cylinder
$X$	= complex amplitude of the excitation force
$W$	= width of the Duck
$Z$	= radiation impedance
$Z_B, Z_H$	= vertical distances of the centre of mass of the ballast and hull measured from the centre of the cylinder
$Z_{CM}$	= vertical distance of the centre of mass of the system measured from the centre of the cylinder

## The Edinburgh Duck

In 1974 Salter described his invention at the University of Edinburgh of a promising new wave energy converter (WEC) [1]. By the early nineteen-eighties this device, which is now generally referred to as the Edinburgh Duck, had been extensively studied. A feature of the early work was the development of ‘reactive’ control techniques with power capture efficiencies of over 80% being demonstrated across a wide range of wave periods in wave tank tests of one-hundredth scale models [2, 3]. Later, through the experimental implementation of a form of ‘complex conjugate’ control, Nebel was able to show the potential for further productivity improvements [4].

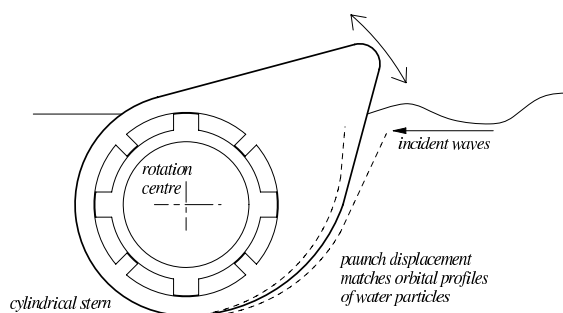


**Figure 1:** Duck profile (adapted from [1]) showing early spline-pump power-take-off concept.

The original design of the Duck was based on the efficient hydrodynamic shape that is shown in Figure 1, which was able to rotate about an axis parallel to the incident waves. Many Ducks would be laid in ‘terminator’ arrays across the prevailing wave direction and energy would be captured from their movements relative to a common cylindrical ‘spine’. By averaging the reactions from differently-phased Duck motions, the relatively stationary and torsionally-stiff spine would thus provide a common source of reaction for the many separate electricity generating systems. A contemporary artist’s impression of a Duck wave-farm is shown in Figure 2.

To relieve excessive heave and surge bending moments, the spine for a complete Duck power station evolved over a number of years into an articulating linear array of separate closed tubes that were interconnected by active two degree-of-freedom joints. During experimental studies it was found that useful additional wave energy could be captured from the

movements of these joints [2]. Typical dimensions for a single 2 MW Duck, designed to match the North Atlantic conditions, were 10 to 15 m stern diameter and 20 to 30 m wide. Some references to the Duck’s articulated-spine are evident in the recent sea-going machines built by Pelamis Wave Power.



**Figure 2:** An early artist’s impression of a Duck string [3]

Early Duck designs were driven by the UK wave energy program which required the development of 2 GW power station concepts and so part of the philosophy behind the spine-mounted terminator concept was to maximise the use of sea-space. Because the reaction-forces required for the power generation were provided for within the complete floating system, Duck-strings could be ‘slack-moored’ so that the seabed attachments would be required only to provide against mean drift forces.

During the nineteen-eighties, a float-alone 2MW solo Duck was studied [5, 6]. It offered a possible route to the kind of experience in design, construction and operation of sea-going systems that would be helpful in the development of 2GW systems. In contrast to the slack-moored Duck-string, the spine-less solo Duck shown in in Figure 3 (one of several possible configurations) would be connected by a tension-leg arrangement to piled seabed attachments that would also provide reaction forces for its power-take-off system.

Tank experiments with a solo Duck, however, subsequently showed that it would be hard to prevent unacceptable snatching of its tension-leg cables. In steep waves these would at times go completely slack, and then violently tighten again when the hydrodynamic loads reversed again.

The tension-leg cables of the solo Duck design were therefore replaced by post-tensioned concrete tubes, referred to as *struts*. Compared with the unavoidable stress-reversals of the steel cables within the tension-leg system, the steel bars within the struts would remain always in tension and would therefore be protected against fatigue. The struts of the solo Duck would be connected by a universal-joint to the seabed attachments to give the machine the freedom to automatically align

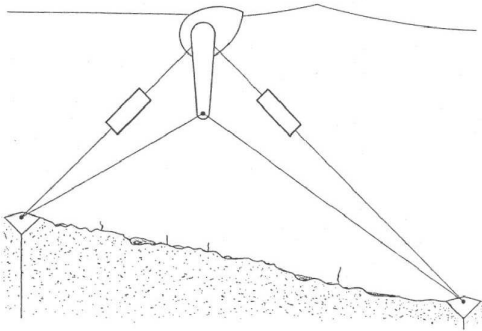


**Figure 3:** A solo Duck with tension-leg moorings and piled seabed attachments from [6]. In this particular arrangement, the arm and the lower lines provide torque reaction for the Duck power-take-off system whilst the boxes in the upper lines contain hydraulic mechanisms for yielding and elasticity control.

with the predominant direction of the incident waves and swell. Details of this design can be found at [7].

In this paper a further development of the solo Duck is considered, in which the power-take-off has been modified to produce fresh water in place of electricity.

The *desalination Duck* uses wave induced motions to directly drive a vapour-compression desalination process. This system is particularly accessible to study because the vapour-compression process has a force characteristic that is very close to the classic linear damping which is usually assumed in frequency domain mathematical work. A brief description of the system is given below, whilst a more detailed treatment can be found at [7, 8].

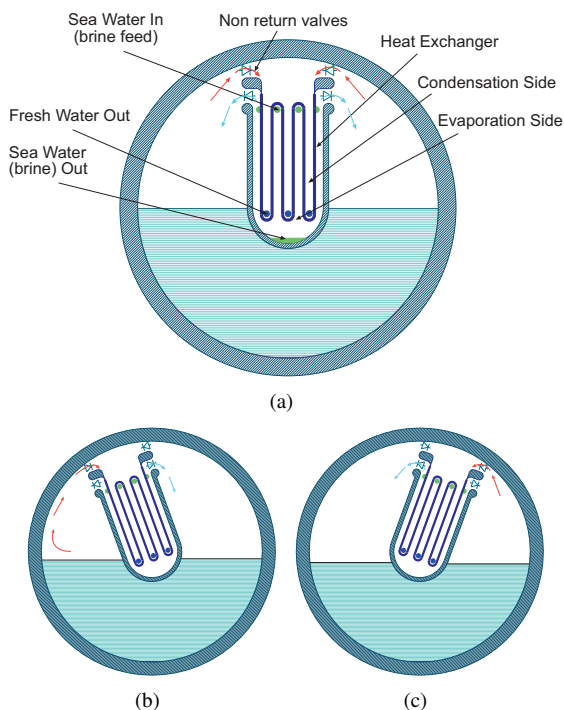


**Figure 4:** Schematic section of the desalination Duck

In the desalination Duck, which is sketched in Figure 4, instead of the turbo-compressor used in most vapour compression systems, the pumping action is provided directly by the motion of the Duck in waves. The body of the Duck is partially filled with warm water at almost boiling temperature and a central partition divides the interior into two separate steam compartments with interconnecting valves. While the Duck undergoes its wave-driven alternating rotations, the water-pendulum tends to stay relatively fixed and so the system forms an enormous, positive displacement double acting pump with no sliding seals or accurate machined parts and very low internal losses. The torque opposing the wave motion of the Duck is proportional to the pressure across the partition which, being proportional to the angular velocity, provides something like the ideal linear damping.

The warm sea water feed falls downwards along a surface of the heat-exchanger and is evaporated by the reduction of pressure in the suction chamber, drawing latent heat from the heat-exchanger. On the next stroke, compression occurs and warms the vapour. The warm pressurised vapour is then fed to the other cooler side of the heat-exchanger where condensation occurs with release of the latent heat. By sequencing the non-return valves shown in Figure 4 the vapour is directed alternately through the compression and suction sides of the heat-exchanger which is folded in a series of clamped U-shapes in such way as to provide the separation surface for the process.

It will be noted that the desalination Duck discussed here is circular in section rather than Duck-shaped. This design change followed numerical hydrodynamic modelling studies that sought to simplify the Duck profile in order to offer cheaper construction without significantly changing its wave energy absorption capability. Attention was focused on a cylinder with an off-centre axis of rotation. The modelling was carried out using the linear Boundary Element Method package: *WAMIT*. In addition to the implicit assumptions of linear potential flow this model comprised a three degrees-of-freedom equation of motion (in surge, heave and pitch) in which the rigid mooring struts were represented by the inclusion of an external stiffness matrix.

Hydrodynamic coefficients, excitation forces and motions, based on a linear-damping control strategy, were computed for different positions of the axis of rotation and for different submerged volumes. Details on this study can be found in [9].

Figure 5 shows a comparison of the performance obtained for the 'classic' solo Duck and for the cylindrical Duck with off-centred axis. A plot of tank measurements obtained by Skyner [5] in regular waves using optimum spring and damping control forces in heave, surge and pitch for the classic Duck is also included to put into context the reduced bandwidth that occurs when only damping is used as control force. As this was a first-try of the cylindrical device without any attempt having been made to optimise its performance,

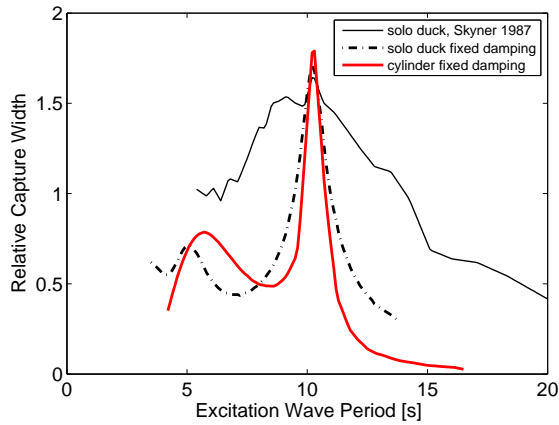


**Figure 5:** Performance comparison in regular waves between two varieties of the ‘classic’ solo Duck and the cylindrical version with off-centred axis of rotation that is discussed in this paper. The thin upper line shows tank measurements by Skyner [5] for a classic Duck using frequency-specific mixes of spring and damping in pitch, surge and heave. The other two lines correspond to numerical-models of the classic duck and of the cylindrical duck using frequency-specific optimal damping (results from [9]). All curves were scaled such as to place the curve peaks at 10 s to bring them into line with the notional centre of the North East Atlantic spectral regime. *Relative Capture Width*, a term commonly used by wave energy engineers, refers to the ratio of the power captured by the device to that incident upon its width (see equation(10)).

this comparison with a mature classic duck was not felt to be too discouraging.

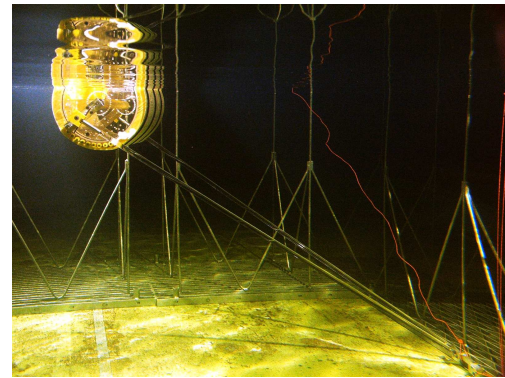
### Tank tests with a 1/33 scale model

To validate the numerical model, a 1:33 scale model was built. The main structural components were made of clear acrylic material to allow easy viewing of the behaviour of the inner mass of water, and confirmation that it was working as a positive displacement double acting pump. It was provided with a mechanism to allow changes in the position of the axis of rotation as well as an array of steel-rods that could be removed allowing an easy variation of mass.

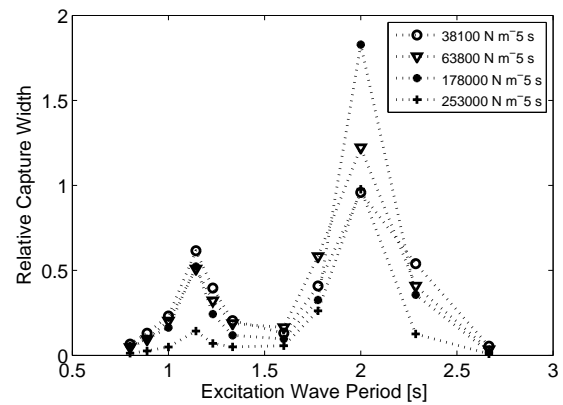
The model was connected to the mooring system through two rigid struts shaped as a "V" yoke, which connected each end of the cylinder-axis to a fixed tank floor attachment through a modified universal joint. This arrangement allowed the system to yaw and to follow changing tank sea-states. Figure 6(a) shows a fish-eye view of the model during tests.

The steam desalination unit of the proposed full-scale device was represented in the tank model by an air-damper that was designed to impose a pressure-difference across the central partition that would be proportional to the angular velocity of the cylindrical Duck.

The initial damper design used a pre-calibrated synthetic felt material which was fitted into the partition. The particular material was chosen because of the known



(a)



(b)

**Figure 6:** (a) Fish-eye view of the 1:33 scale cylindrical model with offset axis under test in the Curved Tank at the University of Edinburgh. (b) Measured performance in small amplitude regular waves with different nominal damping values. Eleven different wave periods were used.

relatively linear relationship between the pressure drop across it and the flow through it. Previous studies had used a similar material when working with oscillating water column models [10]. Sadly it was found that the calibrated characteristics of this material were only valid whilst the felt was dry, and that very small quantities of entrained water would greatly change it.

The damper was re-designed with the synthetic felt material replaced by thin stainless-steel shims with slit cuts that were found to induce pressure-drops proportional to flow-rate. Damping rates were varied by selecting shims that had different stiffnesses (a function of the length of the slit cuts). Details about the methodology used to calibrate the damper can be found at [11].

From the calibration curves for each set of shims that were used, the relationship was known between the pressure differential across the partition and the flow through it. The instantaneous pneumatic power absorbed by the tank model could therefore be estimated from knowledge only of the pressure differential across the partition.

The tests took place at the Edinburgh Curved tank and

details on the methodology can also be found at [11]. Figure 6(b) shows the measured performance from these tests, plotted as relative capture width, in regular waves of eleven different periods and for four different nominal damping values.

### Simplified one degree-of-freedom model

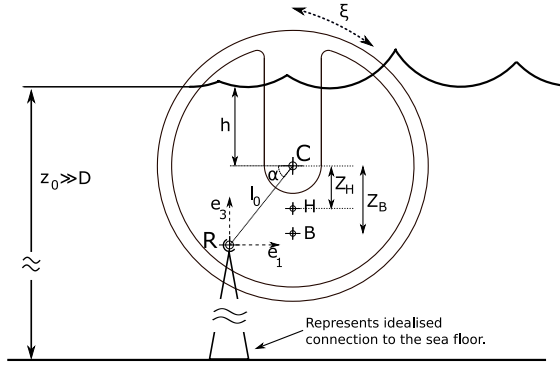


**Figure 7:** Schematic drawing to introduce the nomenclature of the one-degree-of-freedom model.

In this section a simplified analytic model of the modified Duck is discussed. The hull of the Duck is a horizontal cylinder piercing the water surface at a certain draft  $h$ . The cylinder can rotate around an off-centred axis of rotation located at point R (see Figure 7). The water depth is  $z_0$ . Only one-degree-of-freedom is assumed and point R is fixed in space. Because there is no compliance in heave and surge it is expected that the performance will drop. The power-take-off is assumed to be linear and taken at point R. The water pendulum is neglected.

*WAMIT* is used to compute the excitation forces, hydrodynamic coefficients and hydrostatic stiffness (at point R) so all the linear potential flow theory assumptions apply as well: the flow is incompressible, inviscid and irrotational and only small amplitude incident waves and small motions are considered.

The geometrical dimensions of the 1:33 scale model are taken into account as the geometrical inputs. Full scale dimensions can be derived by multiplying by scale factors derived through a Froude scale similarity law. Table 1 show the geometrical dimensions of the 1:33 scale model and the respective full scale values.

Two right-handed coordinate systems with origin at point R are considered. One which is fixed in space and associated with an inertial frame of reference, with base vectors given by  $\{\vec{e}_1, \vec{e}_3\}$  (represented in Figure 7) and a second coordinate system fixed with the body, given by the base vectors  $\{\vec{b}_1, \vec{b}_3\}$  (not shown in Figure 7). Furthermore the two coordinate systems are coincident when the body is at rest in still water [12, § 6.15].

The angular displacement between the two coordinate systems is an harmonic function of time represented by  $\xi$  (in rad). Using complex representation, this is given

Physical Quantity	Variable	Value	Factor	Full scale
Water Depth	$z_0$	1.2 m	33	40 m
External diameter	$D$	0.364m	33	12m
Displaced water volume ratio	$\forall/V$	0.70	1	0.70
Total mass	$\rho \forall$	46.6kg	$(33)^3$	1673t
Wave Period	$T$	0.35 – 3.0s	$\sqrt{33}$	2.0 – 17.0s

**Table 1:** Geometrical dimensions of the 1:33 scale model used to compute the excitation forces, hydrodynamic coefficients and hydrostatic stiffness and respective full scale values (obtained through multiplicative factors derived following Froude similarity laws).

by:

$$\xi = Re\{\hat{\xi} \exp(i\omega t)\} \quad (1a)$$

where  $\hat{\xi}$  is a complex amplitude. The velocity and acceleration are respectively given by:

$$u(t) = \dot{\xi} = i\omega \xi \quad (1b)$$

$$\dot{u}(t) = \ddot{\xi} = -\omega^2 \xi \quad (1c)$$

The one-degree-of-freedom equation of motion can be written as:

$$J_{22} \ddot{\xi} = f_d + f_h \quad (2)$$

where  $J_{22}$  represents component in the direction of  $\vec{b}_2$  of the inertia matrix. The power take off moment ( $f_d$ ) which is assumed more generally to be linear is given by:

$$f_d(t) = -K_0 u(t) \quad (3)$$

and  $f_h = f_x + f_r + f_c$  the hydrodynamic forces, which in the linear theory can be separated into two main components: the excitation force ( $f_x$ ) and the radiation force ( $f_r$ ) [12]. The hydrostatic component ( $f_c$ ) is also included here as part of  $f_h$ :

$$f_x(t) = Re\{AX e^{i\omega t}\} \quad (4a)$$

$$f_r(t) = (\omega^2 a_{55} - i\omega b_{55}) \xi \quad (4b)$$

$$f_c(t) = -c_{55} \xi \quad (4c)$$

where  $X$  is the complex amplitude of the exciting force proportional to the (small) amplitude of the exciting wave  $A$ .  $\omega$  is the angular frequency of the exciting wave. The coefficients  $a_{55}$  and  $b_{55}$  are function of  $\omega$  and are commonly known as the added mass and hydrodynamic damping ( $a_{55}$ ,  $b_{55}$  and  $c_{55}$  are obtained through *WAMIT*).

Substituting (4) and (1) into (2), the equation of motion can then be written as:

$$(Z + K_0) U = AX \quad (5a)$$

where  $Z$  is the radiation impedance, given by:

$$Z = i\omega \left( J_{22} + a_{55} - \frac{c_{55}}{\omega^2} \right) + b_{55} \quad (5b)$$

and  $U$  is the complex amplitude of the velocity  $U = i\omega \hat{\xi}$ .

Following Evans [13] the mean power absorbed by the device over an integer number of wave cycles is:

$$\begin{aligned}\overline{P_{abs}} &= -\frac{1}{T} \int_0^T f_d(t) u(t) dt = -\frac{1}{2} \text{Re} \{ F_d^* U \} = \\ &= \frac{1}{4} (K_0 + K_0^*) |U|^2 = \frac{A^2 |X|^2}{8 b_{55}} \left( 1 - \frac{|K_0 - Z^*|^2}{|K_0 + Z|^2} \right)\end{aligned}$$

The maximum mean absorbed power ( $\overline{P_{max}}$ ) that is possible to achieve through a linear power-take-off is obtained when the linear damping matches the complex conjugate of radiation impedance of every incoming wave, i.e., when  $K_0 = Z^*$ . Such control strategy is commonly referred as complex conjugate control and it implies the constant adjustment of the damping and spring terms of the control force to match the hydrodynamic added mass and damping which are strongly dependent on the wave period.  $\overline{P_{max}}$  is then given by:

$$\overline{P_{max}} = \frac{A |X|^2}{8 b_{55}} \quad (6)$$

If the control force consists only on pure damping,  $K_0$  is a real number and the mean absorbed power is given by:

$$\overline{P_{abs}} = \frac{A^2 |X|^2}{4 (b_{55} + |Z|)} \left( 1 - \frac{(K_0 - |Z|)^2}{|K_0 + Z|^2} \right) \quad (7)$$

The maximum absorbed power is then achieved when:

$$(K_0)_{opt} = |Z| = \sqrt{\left( \omega (J_{22} + a_{55}) - \frac{c_{55}}{\omega} \right)^2 + b_{55}^2} \quad (8)$$

and is given by:

$$\overline{P_{max}} = \frac{A^2 |X|^2}{4 (b_{55} + |Z|)} \quad (9)$$

A comparison of the optimum performance obtained using linear power-take-off through complex conjugate and pure damping control is presented in Figure 8.

The Relative Capture Width (RCW) is a non-dimensional quantity obtained by dividing by the width of the device an equivalent length for which all wave energy transported in the wave front is absorbed. It is defined as the mean absorbed power by the device ( $\overline{P_{abs}}$ ) divided by the average incident wave power per unit crest length ( $\overline{P_w}$ ), divided by the width of the device ( $W$ ):

$$RCW = \frac{\overline{P_{abs}}}{\overline{P_w} W} \quad (10)$$

$\overline{P_w}$  for regular waves is equal to the average energy density ( $E$ ) multiplied by the group velocity of the wave ( $c_g$ ), and for deep water is given by:

$$\overline{P_w} = E c_g = \frac{\rho g^2 A^2 T}{8\pi} \quad (11)$$

In the case of the desalination Duck, the pure damping is a fixed value chosen in such way to match the most probable wave conditions of the location where the device is meant to be deployed. Figure 8 shows also the performance obtained for fixed values of pure damping.

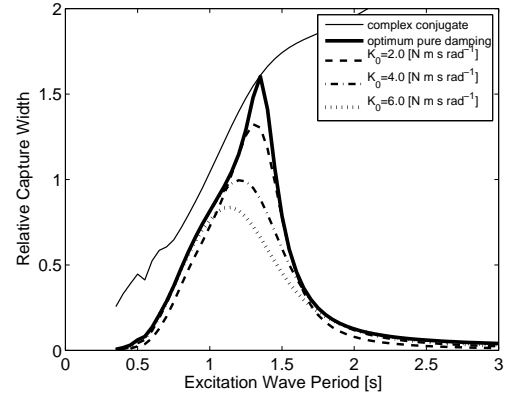


**Figure 8:** Comparison of performances obtained with a linear power-take-off. The continuous thin line is related with the complex conjugate control (when  $K_0(\omega) = Z^*(\omega)$ ), the continuous thick line with pure damping control (when  $K_0(\omega) = |Z(\omega)|$ ), and the broken lines with different values of fixed damping ( $K_0 = 2.0, 4.0$  and  $6.0$  Nms/rad respectively).

### Optimisation of the mass distribution

In this section, the variation of Duck performance with the device inertia is examined, with the total mass being kept constant. Such inertia changes are made by altering the positions of the discrete masses that form the 'ballast' of the Duck. In the real world this knowledge could be used to find the optimum arrangement for a fixed ballast system or it could be used in the control of some non-trivial mechanism which might allow the active re-arrangement of ballast during device operation in order to maximise energy capture.

If the distribution of mass in the device is optimised for a certain wave exciting frequency  $\omega_0 = 2\pi/T_0$ , and the maximum absorbed power is achieved at this particular frequency, then  $|Z| = b_{55}$ , and the maximum mean absorbed power is equal to  $\overline{P_{max}}(\omega_0)$  (given by equation (6) at  $\omega_0$ ). This condition also implies that the optimum inertia would balance the hydrostatic stiffness and hydrodynamic added mass (at this particular frequency,  $\omega_0$ ):

$$J_{22} + a_{55} - \frac{c_{55}}{\omega^2} = 0 \quad (12)$$

Let  $m_B$  be the mass of the ballast and  $Z_B$  the (vertical) distance from its centre of mass to the centre of the cylinder and  $m_H$  and  $Z_H$ , the mass of the hull and the vertical distance from its centre of mass to the centre of the cylinder (see Figure 7).

The (vertical) position of the centre of mass of the system (hull+ballast) is then given by:

$$Z_{CM} = \frac{m_H Z_H + m_B Z_B}{m} \quad (13a)$$

where  $m$  is the total mass of the device:

$$m = m_H + m_B = \text{const.} \quad (13b)$$

The inertia of the device  $J_{22}$  at the rotation point (point R) can be expressed as the sum of the inertias of hull ( $J_H$ ) and ballast ( $J_B$ ):

$$J_{22} = J_H + J_B \quad (14a)$$

The changes in the value of  $J_{22}$  are only due to the variation in the location of the ballast ( $J_H$  is constant).

Using the parallel axis theorem the inertias can be written as:

$$J_H = I_H + m_H d_H^2 \quad (14b)$$

$$J_B = I_B + m_B d_B^2 \quad (14c)$$

where  $I_H$  and  $I_B$  are the inertias of the hull and ballast at correspondent centres of mass and  $d_H$  and  $d_B$  the distances from centre of rotation (point R) to centres of mass of the hull and ballast (point H and B) respectively:

$$d_H^2 = (l_0 \sin \alpha - Z_H)^2 + (l_0 \cos \alpha)^2 \quad (14d)$$

$$d_B^2 = (l_0 \sin \alpha - Z_B)^2 + (l_0 \cos \alpha)^2 \quad (14e)$$

The inertia at the centre of rotation can then expressed as:

$$J_{22} = I_0 - 2m_B l_0 \sin \alpha Z_B + m_B Z_B^2 \quad (14f)$$

where  $I_0$  is a constant term given by:

$$I_0 = I_H + I_B + (Z_H^2 - 2l_0 \sin \alpha Z_H) m_H + l_0^2 m$$

The hydrostatic stiffness  $c_{55}$  is computed by *WAMIT* at the centre of rotation (point R). Following [12, §6.16] it can be written as:

$$c_{55} = \gamma_0 - m g z_g \quad (15a)$$

with:

$$\gamma_0 = g \rho (S_{11} + \forall z_b) \quad (15b)$$

where  $S_{11}$  is the water-plane area,  $\forall$  the total displaced volume of water,  $z_b$  the vertical distance of the centre of buoyancy and  $z_g$  is the vertical distance of the centre of mass (measured from R). The constant  $\gamma_0$  is easily computed as the centre of mass ( $z_g$ ) and the total mass ( $m$ ) of the device are known (given by *WAMIT*).

Noting that the centre of mass  $z_g$  can be expressed as a function of the position of the centre of mass of the ballast through equation (13a), and substituting

$$z_g = l_0 \sin \alpha - Z_{CM} \quad (15c)$$

into (15a), the hydrostatic stiffness can then be rewritten as function of the position of the centre of mass of the ballast:

$$c_{55} = \gamma_1 + g m_B Z_B \quad (15d)$$

where:

$$\gamma_1 = \gamma_0 + g m_H Z_H - g m l_0 \sin \alpha \quad (15e)$$

Substituting (15d) and (14f) into (12) a relation for the optimum position of the centre of mass of the ballast which maximises the absorbed power for a certain exciting wave frequency ( $\omega_0$ ) is obtained:

$$Z_B^2 + b Z_B + c = 0 \quad (16a)$$

with:

$$b = -2l_0 \sin \alpha - \frac{g}{\omega^2} \quad (16b)$$

$$c = \frac{I_0 + a_{55}}{m_B} - \frac{\gamma_1}{\omega^2 m_B} \quad (16c)$$

which as the solution:

$$Z_B = \frac{1}{2} \left( -b \pm \sqrt{\Delta} \right) \quad (16d)$$

with:

$$\Delta = b^2 - 4c \quad (16e)$$

The solutions (16d) are real only if  $\Delta \geq 0$ . This condition can impose a minimum value to the mass of the ballast ( $m_B$ ) such that its position is capable to influence the performance of the device:

$$m_B \geq 4 \frac{1}{b^2} \left( I_0 + a_{55} - \frac{\gamma_1}{\omega^2} \right) \quad (16f)$$

Furthermore, the problem can be simplified by neglecting the water pendulum. If the hull is a perfect symmetric cylinder with homogeneous mass, the centre of mass is at its centre ( $Z_H = 0$ ) and simplified expressions for  $I_0$  and  $\gamma_0$  are obtained. If the masses of the hull and ballast are parametrised as  $m_H = x m_B$ , the total mass of the device is given by:

$$m = \forall \rho = m_H + m_B = (1+x) m_B \quad (17a)$$

and the inertias of the hull and ballast are expressed as:

$$I_H = m_H (D/2)^2 = x m_B (D/2)^2 \quad (17b)$$

$$I_B = m_B K_B^2 \quad (17c)$$

where  $D$  is the external diameter of the cylinder and  $K_B$  the radius of gyration of the ballast,

$$\frac{I_0}{m_B} = x \left( (D/2)^2 + l_0^2 \right) + K_B^2 + l_0^2 \quad (17d)$$

$$\frac{\gamma_1}{m_B} = (1+x) \left( \frac{\gamma_0}{m} - g l_0 \sin \alpha \right) \quad (17e)$$

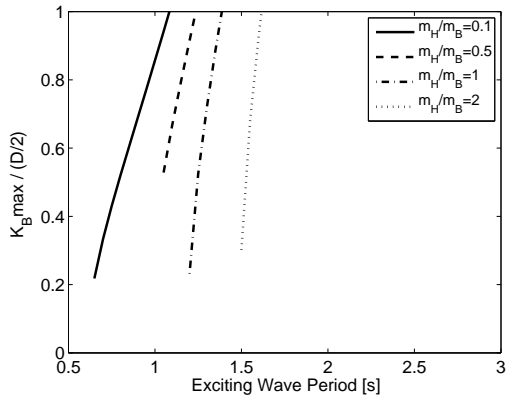
and substituting in (16f) the condition for  $m_B$  can be rewritten as:

$$m_B \geq \frac{\frac{4}{b^2} a_{55}}{1 - \frac{4}{b^2} \left( \frac{I_0}{m_B} + \frac{\gamma_1}{m_B \omega^2} \right)} \quad (17f)$$

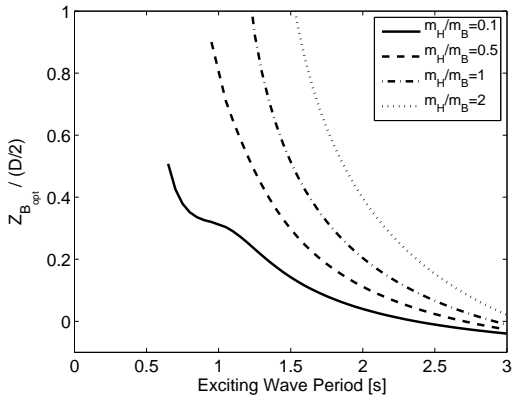
In order to have a positive mass ( $m_B > 0$ ), it is necessary that the denominator of equation (17f) stays positive. This implies the following condition for the radius of gyration of the ballast:

$$K_B^2 < \frac{b^2}{4} - x \left( \left( \frac{D}{2} \right)^2 + l_0^2 \right) - l_0^2 - \frac{1+x}{\omega^2} \left( \frac{\gamma_0}{m} - g l_0 \sin \alpha \right) \quad (17g)$$

The dependency of the maximum radius of gyration ( $K_B$ ) for different mass ratios ( $x$ ) with the incident wave period is plotted in Figure 9(a). This graph shows that the mass ratio ( $x$ ) imposes a lower limit in the



(a)



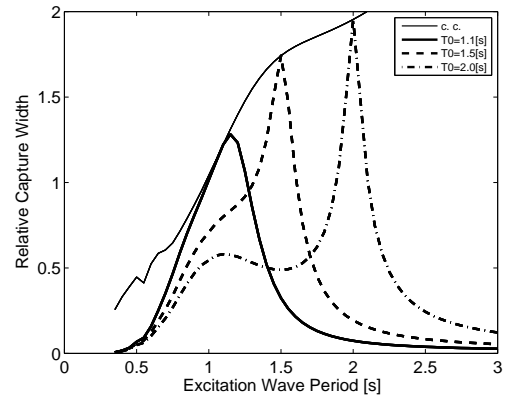
(b)

**Figure 9:** (a) Normalised maximum radius of gyration for the ballast to satisfy condition (17g) for mass ratios given by:  $x = \frac{m_H}{m_B} = 0.1, 0.5, 1, 2$  (b) Normalised optimum location of the centre of mass of the ballast ( $Z_B$ ) which maximises the mean absorbed power for the same mass ratios ( $x$ ) as in (a).

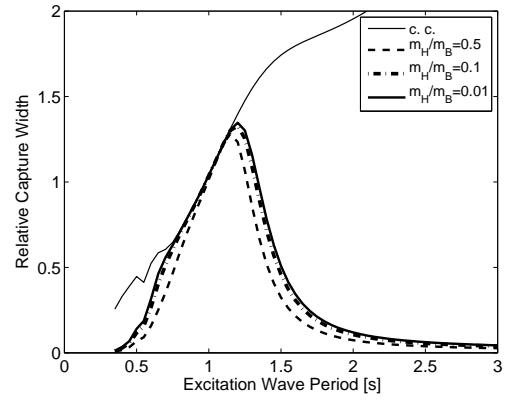
incident wave period which satisfies the condition given by equation (17g). It also implies a limit in the optimum position of the ballast  $Z_B$  which satisfies the maximum mean absorbed power. This is particularly clear in the graph of Figure 9(b).

For a fixed value of the mass ratio,  $x = 0.5$  (i.e.  $m_B = 2m_H$ ), the performances obtained with a pure damping control are re-plotted in Figure 10(a), for different values of  $Z_B$ , chosen to maximise the mean absorbed power for the incident wave periods equal to  $T_0 = 1.1, 1.5, 2.0$ s. The graph shows that by rearranging the ballast distribution the performance of the device changes, and by choosing an appropriate value for  $Z_B$ , the optimum performance of the device for a certain sea state is obtained.

The thick lines in Figure 10(b) show the performances obtained using a pure damping power-take-off when different mass ratios are considered. The value of  $Z_B$  is the same for all curves and was chosen to maximise the mean absorbed power for  $T_0 = 1.1$ s. It can be observed an increase in the performance when the mass ratio  $x = m_H/m_B$  decreases. The increase in performance is asymptotic and tend to a maximum for a mass ratio



(a)



(b)

**Figure 10:** The thin continuous line is associated with complex conjugate control while the thick lines are obtained using optimum pure damping control. (a) The optimum pure damping curves are obtained for different locations of the ballast chosen to maximise the mean absorbed power at periods  $T_0 = 1.1, 1.5, 2.0$ s. The position of the ballast is respectively  $Z_B = 118, 54$  and  $20$  mm. The mass ratio is fixed and equal to  $x = 0.5$  (i.e.  $m_B = 2m_H$ ) (b) The optimum pure damping curves are obtained for a particular location of the ballast ( $Z_B$ ) for different mass ratios  $x = 0.01; 0.1; 0.5$  (i.e.  $m_B = 100m_H, m_B = 10m_H$  and  $m_B = 2m_H$ ).

which has an unrealistic value. But it implies the existence of an optimum value which should be weighted with some design restrains.

## Conclusions

This paper presents the latest studies performed at the University of Edinburgh with a new design for the Duck Wave Energy Converter. Its characteristic cam shape was redesigned as a cylinder with an off-centred axis of rotation. A numerical hydrodynamic model showed that performance broadly similar to that of a conventionally shaped Duck might be possible. An advantage of the new design should be a reduction in manufacturing cost. The results were applied to a particular version which has a fixed pure damping power-take-off, the *desalination* Duck. In this version, the motion of the device in the waves is used to drive a thermal process

known as vapour-compression and to directly produce fresh water.

To validate the numerical model a 1:33 scale model was built and is currently being tested in the Edinburgh Curved tank. In this scale model the desalination unit was represented by a variable damper.

The performance obtained from the latest tank tests with regular waves and for different values of fixed damping is presented in Figure 6(b). Clearly it shows two maximum performance peaks at periods  $T_0 = 1.2, 2.0$ s (1:33 scale) with the highest reaching a relative capture width of about 1.8. A consistent drop in performance between the two peaks is also observed and can be partially explained as a consequence of energy losses due to drag around the sharp edges of the cylinder. Extensive vortexes are observed around the edges as soon as the model starts to move.

The second part of the paper deals with a simplified model which has only one degree-of-freedom. *WAMIT* is used to compute the excitation forces and hydrodynamic coefficients and so all linear potential flow assumptions apply. The water pendulum and of the rigid strut mooring is neglected. A linear-power-take-off is considered at the centre of rotation of the cylinder. The equations for maximum mean absorbed power are applied and a comparison of performances obtained with fixed damping, optimum pure damping and complex conjugate control is shown in Figure 8. By assuming the existence of a mechanism that is capable of changing the location of ballast in the device, an analysis of the mass distribution is performed. It is shown that by rearranging the ballast distribution the performance of the device is changed and by choosing an appropriate value for the centre of mass of the ballast is possible to optimise the performance of the device for a certain sea state (Figure 10(a)). Moreover, it is shown that the ballast/hull mass ratio has an impact in the performance of the device which tends asymptotically to a maximum (Figure 10(a)).

## Acknowledgements

The first author gratefully acknowledges the a doctoral training support from the University of Edinburgh. The authors would like to thank for the positive contribution and support given by David Forehand, Gareth Gretton, Grégory Payne and Rémy Pascal.

## References

- [1] Stephen H. Salter. Wave power. *Nature*, 249(249):720–724, 1974.
- [2] Stephen H. Salter. Recent progress on ducks. *IEE Proceedings A: Science, Measurement & Technology*, 127(5):308–319, 1980.
- [3] Stephen H. Salter, David C. Jeffrey, and Jamie R.M. Taylor. The architecture of nodding duck wave power generators. *Naval Architect*, -:21–24, January 1976.
- [4] Paul Nebel. Maximizing the efficiency of wave-energy plants using complex conjugate control. *Proc. IMechE Part I - Journal of systems and control engineering*, 206(4):225–236, 1992.
- [5] David Skyner. Solo duck linear analysis. Technical report, University of Edinburgh, 1987.
- [6] Stephen H. Salter. World progress in wave energy-1988. *International Journal of Ambient Energy*, 10(01):3–24, 1989.
- [7] Stephen H. Salter, João Cruz, Jorge Lucas, and Remy Pascal. Wave powered desalination. In *International Conference on Integrated Sustainable Energy Resources in Arid Regions*, Abu Dhabi, 2007.
- [8] Stephen H. Salter. High purity desalination using wave-driven vapour compression. In *Proc. World Renewable Energy Conference*, Aberdeen (UK), 2005.
- [9] João Cruz and Stephen H. Salter. Numerical and experimental modelling of a modified version of the Edinburgh Duck wave energy device. *Proc. IMechE Part M - Journal of Engineering for the Maritime Environment*, 220:129–147, 2006.
- [10] Y. M. C. Delaur and A. Lewis. 3D hydrodynamic modelling of fixed oscillating water column wave power plant by a boundary element methods. *Ocean Engineering*, 30(Issue 3):309–330, February 2003.
- [11] Jorge Lucas. Update on the design of a 1:33 scale model of a modified edinburgh duck wec. In *Proceedings of Offshore Mechanics and Arctic Engineering 2008*, page 11, Estoril, Portugal, June June June 2008.
- [12] John Nicholas Newman. *Marine Hydrodynamics*. The MIT Press, 1977.
- [13] D.V. Evans and C.M. Linton. Hydrodynamics of wave-energy devices. Technical report, University of Bristol, Department of Mathematics, June 1993.

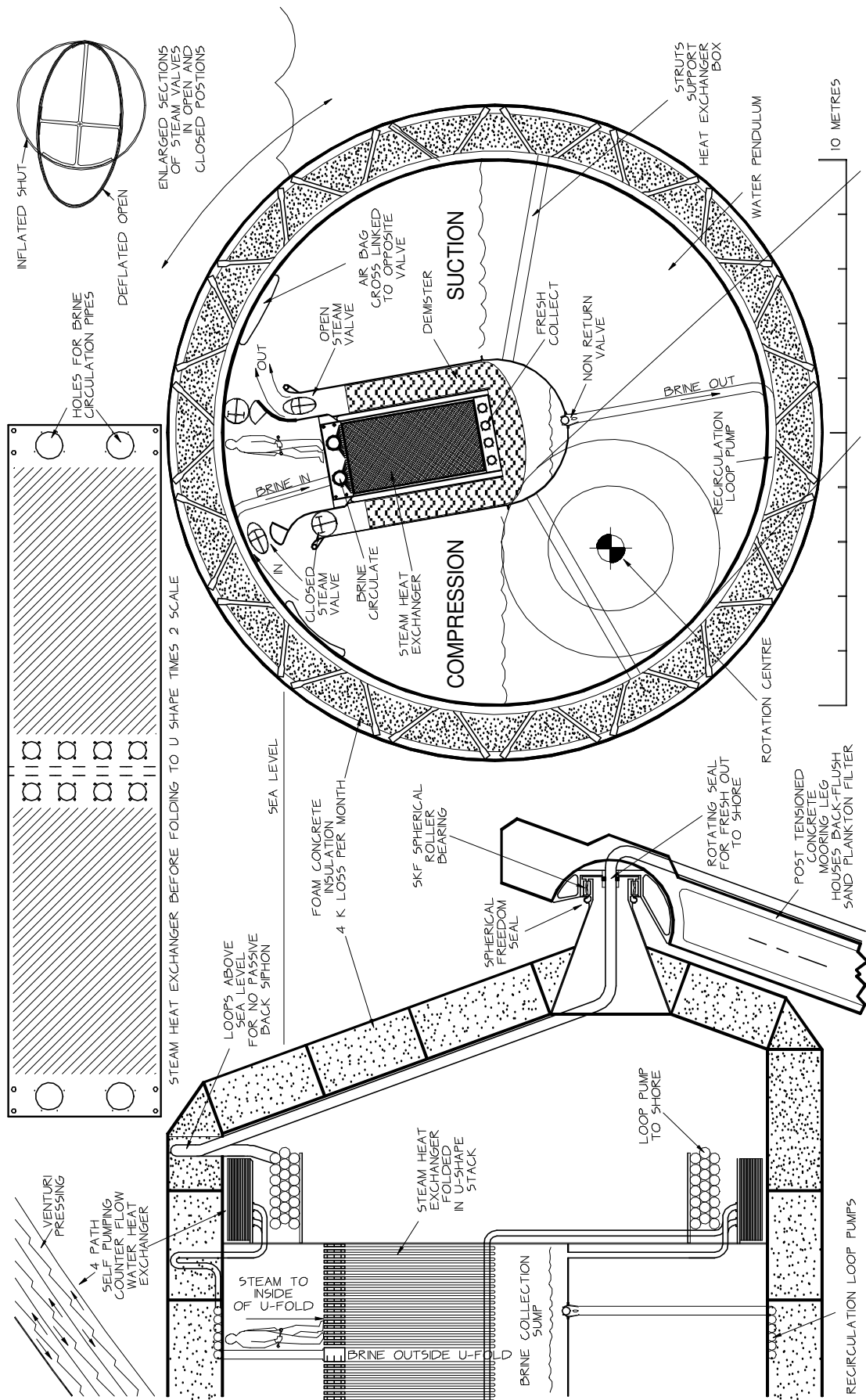


**Figure 11:** Section Through the modified desalination Duck. People would not be present during operation!